phys. stat. sol. (c) **5**, No. 12, 3846–3849 (2008) / **DOI** 10.1002/pssc.200780150

physica status solidi c
www.pss-c.com
current topics in solid state physics

A real time fingerprint identification system based on the AFS8600 sensor and the C6713 DSP processor

K. Tselios, E. N. Zois*, N. A. Livanos, and A. Nassiopoulos

Recearch and Development Telecommunications Laboratory, Department of Electronics, School of Applied Science, Technological and Educational Institution of Athens, Agiou Spiridonos Str., 12210 Aegaleo, Hellas

Received 19 November 2007, revised 12 May 2008, accepted 12 May 2008
Published online 16 September 2008

PACS 07.07.Df, 85.30.De

* Corresponding author: e-mail elias@ee.teiath.gr, Phone: +30 210 5383 383, Fax: +30 210 5385 304

In this paper, a fingerprint pre-process and identification algorithm is implemented using the TMS320C6713 DSP starter kit (DSK) module, along with the Authentec AFS 8600 fingerprint sensor. *Database:* Acquisition is performed using a solid state sensor. The sensor postulates emerge from the theory of the Electric Field technology. *Method*: Images are first subjected to a frequency and orientation processing. This is achieved using Gabor-based filters. This processing has been optimized and implemented on the DSP system. A new method has been developed in order to extract the feature vector of the fingerprint image. A grid, centered at the core-point of the image, is applied to the fingerprint image in order to derive local information. Classification algorithms are developed, which include training as well as evaluating phase. The types of classifiers used were based on the Bayesian approach along with the K-nearest neighbour. *Results:* An identification accuracy of 90% was achieved which is comparable to other procedures described in the literature. *Conclusion:* The combination of a fingerprint processing and identification algorithm using a low cost sensor and DSP module has been presented.

1 Introduction Fingerprint identification is one of the most important and efficient techniques used for biometric recognition. It is one of the most widely-used personal identification measurements or biometrics, because they employ non invasive acquisition methods along with the use of a low cost sensor [1]. A fingerprint is the pattern of ridges and valleys on the surface of it [2]. This surface is initially formed in the living subdermal tissue just below the visible outer layer (dead cells). Fingerprints are anatomic features that are unique to the individual human. Even monozygotic (identical) twins have fingerprints that differ from one another in the same degree that they differ from any other unrelated individual [3]. An important matter is the fingerprint acquisition technology. Some popular technologies are ink-on-paper, optical fingerprint scanning, solid state capacitive sensing, direct thermal-optical scanning, LCD thermal-optical scanning and solid-state active array sensing [3]. A number of techniques have been presented in order to describe a model for fingerprint identification systems [4-8].The present development uses solid-state active array sensing that is based on electric field RF imaging techniques. The model of sensor is the Authentec AFS 8600. This sensor combined along with the TMS320C6713 DSP starter kit (DSK) module results a real time identification system. An identification algorithm has been developed with minimum operator intervention. The preprocessing step includes a number of digital filters for enhancing digital fingerprint images. Gabor based techniques have shown good performance for fingerprint image enhancement and assist to the implementation of feature and minutiae extraction algorithms. The present work describes a new feature for fingerprint identification, based on line directionality [9]. First normalization is applied in order to increase the contrast between ridges and valleys of the fingerprint image. Second, the values of ridge's orientation of subareas of the image is extracted with the implementation of the least square orientation estimation algorithm, which is commonly used in fingerprint

images for orientation estimation. Then in the same subareas, frequency estimation takes place [2]. After, each subarea of the image is filtered using Gabor techniques [10]. After preprocessing, detection of curvature technique (DC) locates the core point of the fingerprint image in order to derive local information, due to the hypothesis that the most precious biometric information is located near the core point [11]. Thirdly a new feature, based on line directionality, is extracted [9]. Finally, identification algorithms are developed, including training as well as evaluating phases [16]. In order to obtain results comparable with other fingerprint identification techniques, the method is applied to a new on-line fingerprint database created along with the identification system.

2 Experimental setup

2.1 The sensor The sensor in this work is a semiconductors electric field based sensing which is called Active Array Sensing [3]. The sensor is operates by collecting very small changes in the parameters of the transmitted signals, as the signals are modulated by interaction with the subdermal layer of the skin. The modulated signals are received by a solid-state antenna array that converts the signal variations into a grey-scaled bitmap image which describes the actual fingerprint. When a finger is placed on the sensor it makes physical contact with both the sensor semiconductor substrate upward of Pixel antenna array and the drive ring. Drive ring is an extremely short-range transmitter that couples a small RF signal onto the living subdermal layer of the finger, produced by a excitation generator. The signal on the live skin generates a quasi-static-electric planar field between the finger and a ground plane (excitation signal reference plane) buried beneath the antenna array [3]. The planar field geometries thus generated replicates the shapes of the ridges and valleys of the underlying live skin. Each of the thousands of elements in the matrix antenna array can generate a grayscale dot and so can be thought of as a pixel in a bitmap. The signal from each antenna is read using an amplifier, and then conditioned to a digital representation of the fingerprint image [3]. An important advantage of this technology is the ability to acquire fingerprints on every condition of the finger skin and independently of the fingerprint contaminations such as dust, oil or other causes. This type of sensor can acquire useful information, with enhanced quality, from people with epidermal variances of their fingers, varying from the normal skin tissues, up to a skin that is dry or worn smooth by mechanical abrasion [1, 3]. The sensor resolution is 250 dpi, while the sensor area covers a 96×96 pixels frame in a 8 bit gray-scale depth [12]. In order to create the database, 40 different individuals have been asked to provide their right pointer fingerprint, 20 times each, thus creating a on line database of 800 samples. Figure 1 provides an Active Array Sensor schematic diagram.

2.2 Normalization For every fingerprint image a preprocessing step was followed in order to maximize the amount of useful information. The first step includes normalization of the image to a constant mean M_0 and variance V_0 according to Eq. (1),

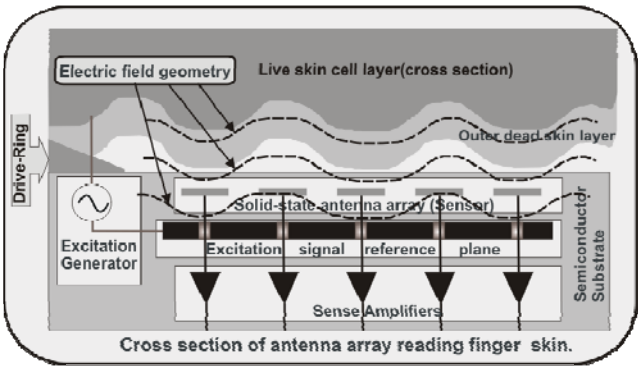

Figure 1 Fingerprint sensor schematic. Cross section of sensor and finger skin [3].

$$N(i,j) = M_0 \pm \sqrt{\frac{V_0 (I(i,j) - M)^2}{V}} \tag{1}$$

were I(i,j) denotes the gray value at pixel (i,j), M and V the estimated mean and variance of image respectively, and N(i,j) the normalized gray level value at pixel (i,j) where the + operator corresponds to the case of having I(i,j) > M [2, 11].

2.3 Ridge orientation estimation The original image has been divided into a 12×12 grid, thus creating 64 subimages. For each subimage the orientation value was evaluated according to the following procedure: Firstly, the gradients $\partial_y(i,j)$ and $\partial_x(i,j)$ were computed at each pixel (i,j) using the Sobel mask [14]. Secondly, local orientation at pixel(i,j) was estimated using the following equations [2, 13]:

$$V_x(i,j) = \sum_{u=i-\frac{w}{2}}^{i+\frac{w}{2}} \sum_{v=j-\frac{w}{2}}^{j+\frac{w}{2}} \partial_x(u,v)^2 - \partial_y(u,v)^2 \tag{2}$$

$$V_y(i,j) = \sum_{u=i-\frac{w}{2}}^{i+\frac{w}{2}} \sum_{v=j-\frac{w}{2}}^{j+\frac{w}{2}} 2\partial_x(u,v) \cdot \partial_y(u,v) \tag{3}$$

$$\theta(i,j) = \frac{1}{2} \cdot \tan^{-1}\left(\frac{V_y(i,j)}{V_x(i,j)}\right) \tag{4}$$

In the above equations, $\theta(i,j)$ is the least square estimate of the local ridge orientation at the block centered at pixel (i,j). Then the orientation values were converted into a continuous vector field by doubling the above $\theta(i,j)$

values as:

$$\Phi_x(i,j) = \cos(2\theta(i,j))\ \ \Phi_y(i,j) = \sin(2\theta(i,j)), \qquad (5)$$

where the vectors $\Phi_x(i,j)$ and $\Phi_y(i,j)$ corresponds to the x and y components of the orientation $\theta(i,j)$. Finally vectors were smoothed for each local area of image, using a mean 5×5 filter. This results to a final estimation of the orientation values O(i,j) at pixel (i,j) [2, 16]:

$$O(i,j) = \frac{1}{2}\cdot \tan^{-1}\left(\frac{\Phi'_y(i,j)}{\Phi'_x(i,j)}\right),$$

where $\Phi'_y(i,j)$ and $\Phi'_x(i,j)$ are the smoothed vectors [2].

2.4 Ridge frequency estimation Each local area in which no minutiae and core points appears, the gray levels along ridges can be modelled as a sinusoidal wave along a direction perpendicular to the local ridge orientation. The frequency of this sinusoidal wave is the local ridge frequency. For every subimage, the projection of the grey-level values along a direction orthogonal to the local ridge orientation has been acquired. This projection forms an almost sinusoidal-shape wave with the local minimum points corresponding to the ridges in the fingerprint [2]. Specifically the number of pixels between consecutive minima (ridges) points in the projected waveform is the value of period T. The ridge frequency f for a block is defined as the inverse of the period T.

2.5 Gabor filtering The ridge orientation and ridge frequency for each local area of the fingerprint image provide useful information which helps in removing undesired noise. Gabor filters were employed because they have frequency and orientation selective properties. These properties allow the filter to be tuned at a specific orientation and frequency according the orientation and the frequency of ridges of the local area of the fingerprint image as described in the previous sections. An even-symmetric Gabor filter in the spatial domain is defined as [10, 11]:

$$G(x,y,:f,\theta) = \exp\left\{-\frac{1}{2}\left[\frac{x_\Phi^2}{\delta_x^2}+\frac{y_\Phi^2}{\delta_y^2}\right]\right\}\cos(2\cdot\pi\cdot f\cdot x_\phi), \qquad (6)$$

$$x_\Phi = x\sin\theta + y\cos\theta,\ y_\Phi = x\cos\theta - y\sin\theta,$$

where θ and f are the orientation and frequency of each subimage, δ_x and δ_y are the standard deviations of the Gaussian envelope along the x and y axes respectively. x_Φ and y_Φ define the x and y axes of the filter coordinate frame, respectively. Figure 2a provides a original fingerprint image while Fig. 2b presents the results of applying the Gabor filters to the normalized subimages. The filtered subimages must be properly thresholded and thinned in order to provide a binary, one pixel wide image [14, 15]. This improves the contrast between the ridges and valleys in a fingerprint image, and consequently facilitates the extraction of feature base on line directionality.

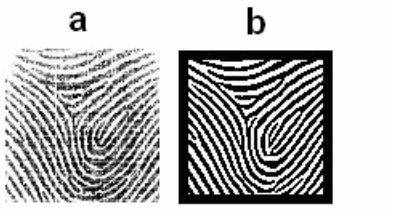

Figure 2 a) Original image. b) Gabor filtered image.

2.6 Feature vector generation Before feature extraction, detection of curvature (DC) was implemented to locate the core point of the fingerprint image [13]. Feature extraction uses a square area of 20 pixels centered at the core point. This corresponds to the most informative section of fingerprint as reported in the literature [13]. The resulting image will be referred to as Binary Thinned Core Point Area (BTCPA). On each pixel (i,j) that is part of BTCPA, a rectangular grid mask with dimensions 3x5 is applied as shown in Fig. 3. Thus, a total of nine positions having a chessboard distance equal to 2 (depicted in the figure as shaded squares) are enabled. The pixels belonging to all two-step paths that connect the reference pixel (i,j) with each D_8 distant pixel (i+k,j+l) are summed in order to create the quantity [9]:

$$f_d(i,j;k,l) = \sum_{\left\{\substack{i+m\\ j+n}\right\}\in \mathrm{BTCPA}} [f_D(i+m,j+n) + f_D(i+k,j+l)]. \qquad (7)$$

Consequently, depending on the combination of k and l, nine similar quantities are formed corresponding to each specific position (i,j). Accordingly, a nine dimensional feature vector is formed by accumulating the above quantity over all (i,j) points of the BTCPA. The nine feature components correspond to the different directions which are defined by the following equation:

$$f_d(k,l) = \sum_{\{i,j\}\in \mathrm{BTCPA}} f_d(i,j:k,l). \qquad (8)$$

Since $f_d(-2,0)$ coincides with $f_d(0,2)$, the f_d feature vector is reduced to a dimensionality equal to 8. The final feature vector can be normalized to the total sum of the extracted parameters in order to obtain a probabilistic meaning.

2.7 Fingerprint identification In this study, we identify fingerprints from a database of 40 different individuals. In order to carry out the identification task, we make use of a K-NN and a Bayesian classifier [16]. In the K-NN case, the unknown feature is classified to the class (individual) with the most numerous nearest neighbors, using a majority vote rule [16]. In the Bayesian approach the classification scheme is described by the following dis-

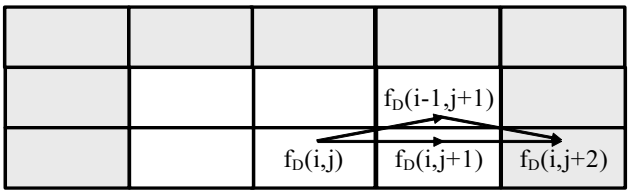

Figure 3 Multiple, two-step paths for accessing the pixel f_d(i,j+2). Shaded pixels have a chessboard distance D_8 equal to 2.

criminant function for each i-class:

$$r_i = \ln(P_i) - 0.5 \cdot \ln|C_i| - 0.5 \cdot ((x - m_i)^T \cdot C^{-1} \cdot (x - m_i)) \quad (9)$$

where x is the unknown pattern vector. Each unknown sample is assigned to one of the classes C_i (i=1,2,3,4,….) associated with the maximum r_i value. P_i expresses the probability of a pattern vector to belong to class I and in this case it is considered equal for all classes. m_i and C_i are the mean value vector and the covariance matrix respectively of class i.

An important parameter of this study was the evaluation of K-nearest neighbour and Bayesian Classifier. In order to create the training and testing patterns we have used 17 samples from each individual for training and the 3 samples for testing. When the K-nearest neighbour classifier is employed, the identification results provide a success rate of 91 percent. This is the case in which 8 nearest neighbours (K = 8) are considered. Identification accuracy does not improve, as an increasing function of the number of neighbours. It is observed that there exists an optimal identification success rate value when K assumes the value of eight. The Bayesian classifier results also in an accuracy of 90.5 percent for P_i = 0.5. The total processing time, ranging from the acquisition of the fingerprint up to the identification results, is about 0.745 seconds when the DSK is employed. The implementation of the procedure in the DSK kit includes downloading the training samples into the DSK memory along with the associated covariance matrices.

3 Conclusions In this work, a combination of a real-time digital signal processing module along with a solid state fingerprint sensor has been described in order to create an on-line fingerprint identification algorithm. The system has been designed in order to provide a low cost, friendly user environment for financial and high security transactions along with minimal user intervention. Every image has 96x96 pixels in a 250 ppi resolution, at 8-bit gray level. Image processing methods were performed by custom developed software using combination of both C and Matlab programming languages. The feature vector was created using a directional method in order to derive local and semi global information about the fingerprint pixel distributions around the core point. Forty people apart the on-line database which enrols a total of 800 fingerprint images using the sensor. The total classification error is below 10% which is comparable to other approaches reported in the literature.

References

[1] D. Maltoni, D. Maio, A. K. Jain, and S. Pradhakar, Handbook of Fingerprint Recognition (Springer-Verlag, New York, 2003).
[2] L Hong, Y. Wan, and A. K. Jain, IEEE Trans. Pattern Anal. Mach. Intell. **20**, 8 (1998).
[3] Solid-State Fingerprint Detection., Authentec White Paper 2065 Rev. 1.1, 2000.
[4] C. H. Park and H. Park, Pattern Recognit. **38**, 495-503 (2005).
[5] F. A. Afsar, M. Arif, and M. Hussain, Fingerprint Identification and Verification System using Minutiae Matching, National Conference on Emerging Technologies, 2004.
[6] N. K Ratha,, K. Karu, S. Chen, and A. K. Jain, IEEE Trans. Pattern Anal. Mach. Intell. **18**(8), 799-813 (1996).
[7] S. Chikkerur, A. N. Cartwright, and V. Govindaraju, Pattern Recognit. **40**, 198-211 (2007).
[8] D. Maltoni and R. Cappelli, Advance in fingerprint modeling, in press.
[9] E. N. Zois, A. A. Nassiopoulos, and V.Anastassopoulos, Signature Verification Based on Line Directionality, IEEE Conf. on Signal Processing Systems, SIPS-05, Athens, Greece, 2005.
[10] W. K. Pratt, Digital Image Processing (Wiley-Interscience, New York, 2001).
[11] A. K. Jain, S. Prabhakar, L. Hong, and S. Pankanti, IEEE Trans. Image Process. **9**(5), 846-859 (2000).
[12] AFS8600 Fingerprint Sensor Daughtercard, Technical Reference. Authentec Inc., 2004.
[13] A. R. Rao, A Taxonomy for Texture Description and Identification (Springer-Verlag, New York, Inc., 1990).
[14] R. C. Gonzalez and R. E. Woods, Digital Image Processing (Pearson Prentice Hall, New Jersey, 2002).
[15] J. Serra, Image Analysis and Mathematical Morphology (Academic Press, 1982).
[16] R. O. Duda, P. E. Hart, and D. G. Stork, Pattern Classification (Wiley-Interscience, New York, 2000).